# Supplemental Materials

***Molecular Biology of the Cell***

**Kishimoto *et al*.**

# Supplemental Materials

Molecular Biology of the Cell

**Phospholipid flippases and Sfk1 are essential for the retention of ergosterol in the plasma membrane**

Kishimoto *et al*.

**Supplemental Figure 1**

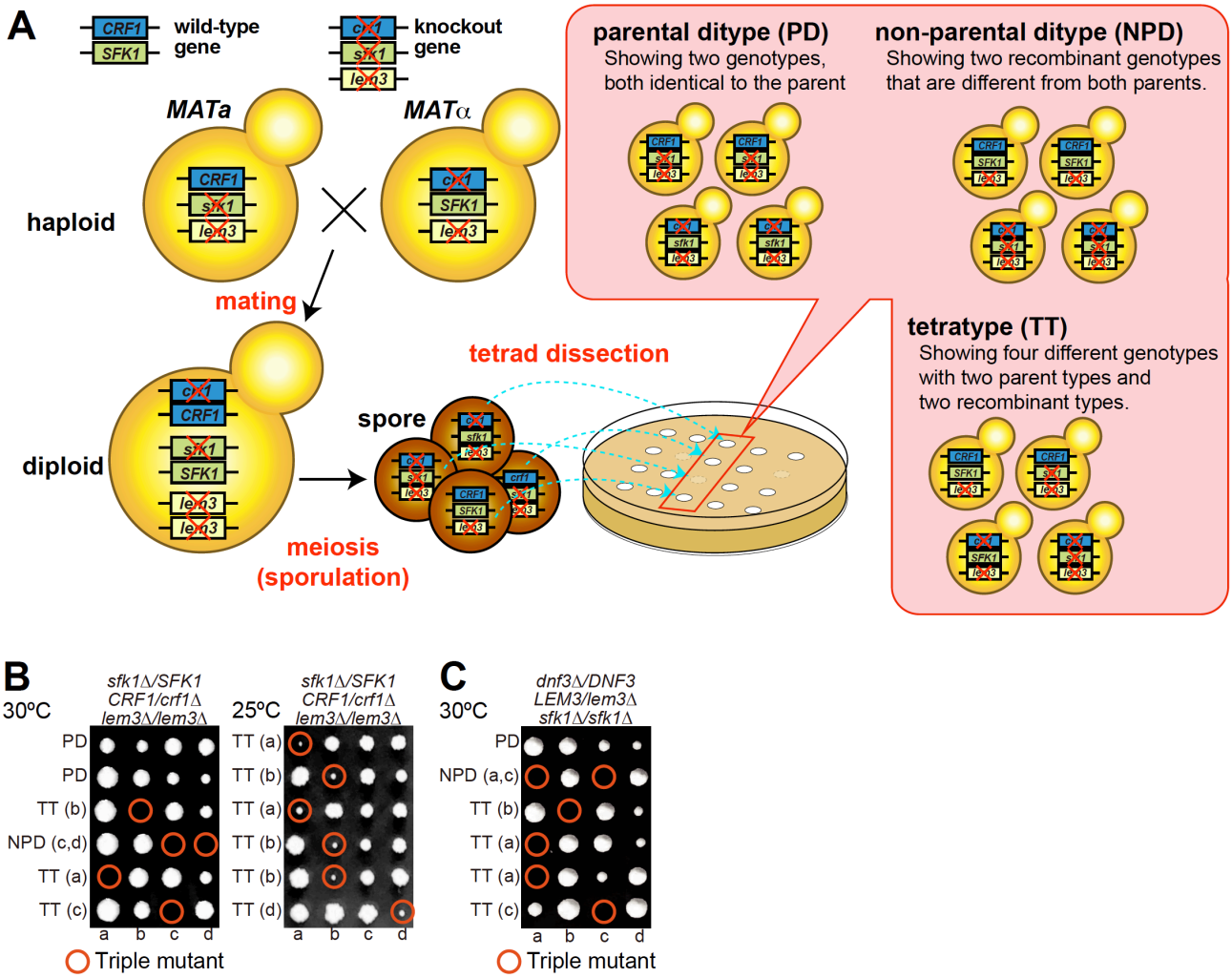


**Supplemental Figure 1.** Tetrad dissection analysis shows the synthetic growth defect of the *crf1*Δ *lem3*Δ *skf1*Δ and *dnf3*Δ *lem3*Δ *skf1*Δ mutants. (A) An illustration of tetrad dissection analysis. (B) Tetrad dissection analysis of the *crf1*Δ*/CRF1 SFK1/sfk1*Δ *lem3*Δ*/lem3*Δ diploid. Cells were sporulated, dissected, and grown at either 30 or 25°C for 4 d. Colonies were replica-plated onto selective media to determine the segregation of the marked mutant alleles. Tetrad genotypes (TT, NPD, and PD) are indicated, and the identities of the triple mutant segregants are shown in parentheses (red circles). (C) Synthetic growth defects of the *dnf3*Δ *lem3*Δ *sfk1*Δ mutant. Tetrad analysis was performed as in (B).

**Supplemental Figure 2**

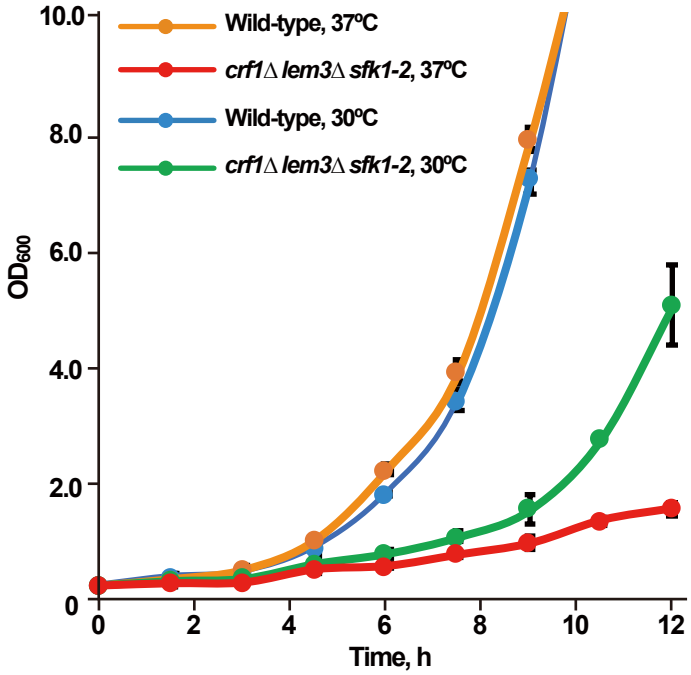


**Supplemental Figure 2.** Growth curves of wild-type and *crf1*Δ *lem3*Δ *skf1-2* cells. Cells were precultured in YPDA medium to the mid-log phase at 30°C. Then, the cells were reinoculated in YPDA at time 0 and cultured at 30 or 37°C. Optical density was measured every 1.5 h. Values represent the mean ± S.D. from three independent experiments.

**Supplemental Figure 3**

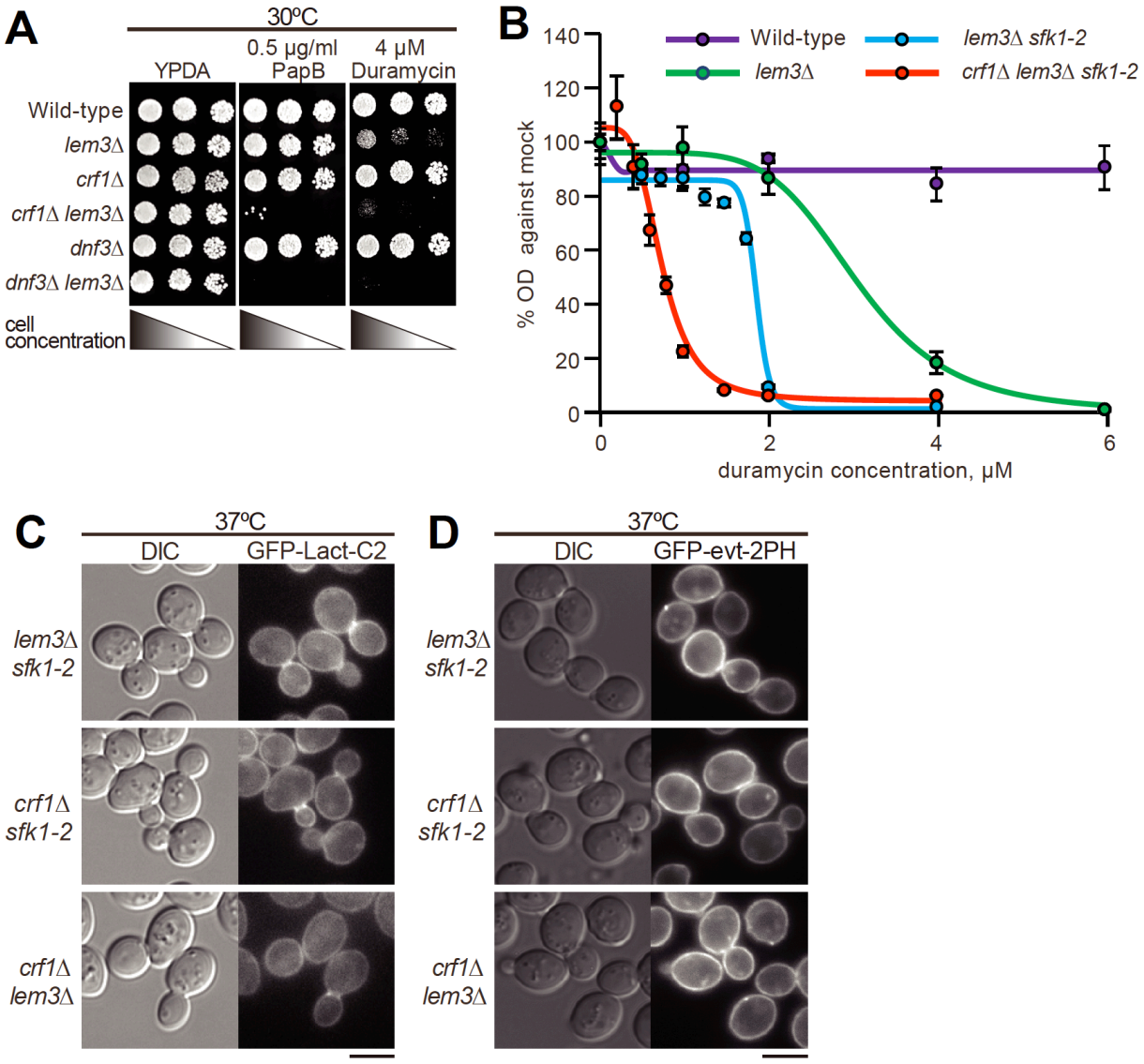


**Supplemental Figure 3.** Phospholipid distributions in the double mutants of *lem3*Δ, *crf1*Δ, *dnf3*Δ, and *sfk1-2* mutations. (A) The *crf1*Δ and *dnf3*Δ mutations increased the sensitivity to PapB and duramycin in the *lem3*Δ mutant. Tenfold serial dilutions of the indicated cell cultures were spotted onto a YPDA plate containing PapB or duramycin, followed by incubation at 30°C for 2 d. (B) The *crf1*Δ *lem3*Δ *sfk1-2* triple mutant showed a higher sensitivity to duramycin in the dose-response curve experiment. The cells were cultured in the absence or presence of indicated concentrations of duramycin for 20 h at 30ºC. Optical density at 600 nm was measured, and the cell growth was plotted as a percentage of the $OD_{600}$ without duramycin. Values represent the mean ± S.D. from five independent experiments. (C) GFP -Lact-C2 was normally localized to the PM in the *lem3*Δ *sfk1-2*, *crf1*Δ *sfk1-2*, and *crf1*Δ *lem3*Δ double mutants. Cells were cultured as in Figure 2E. (D) GFP-evt-2PH was normally localized to the PM in the *lem3*Δ *sfk1-2*, *crf1*Δ *sfk1-2*, and *crf1*Δ *lem3*Δ double mutants. Cells were cultured as in Figure 2E. Bars, 5 µm.

**Supplemental Figure 4**

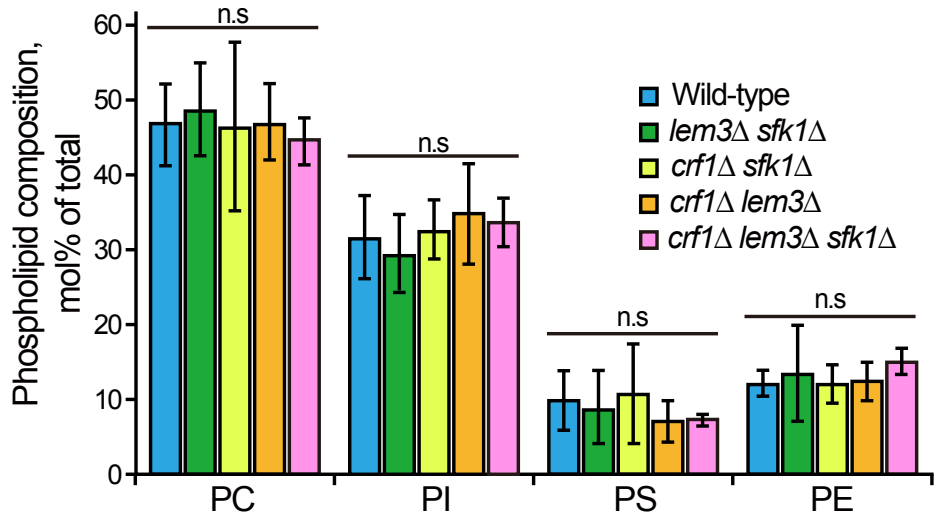


**Supplemental Figure 4.** Analysis of phospholipid composition. PC, phosphatidylinositol (PI), PS, and PE are quantified as a mol percentage of total phospholipids. The data represent the mean ± S.D. derived from the analysis of four to five independent samples. "n.s," indicates no significant difference between all combinations as determined by the Tukey–Kramer test.

**Supplemental Figure 5**

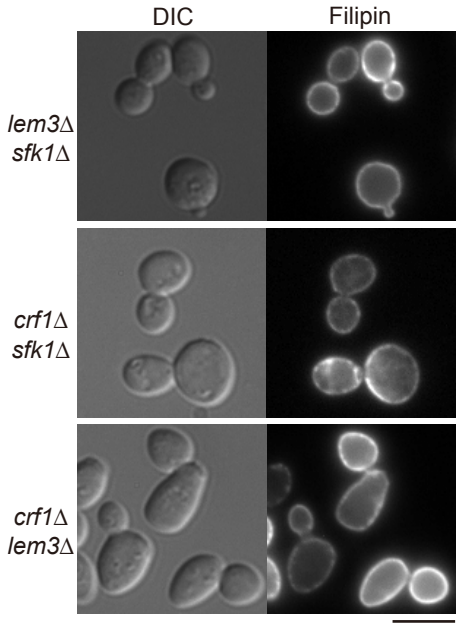


**Supplemental Figure 5.** Filipin staining in the *lem3*Δ *sfk1*Δ, *crf1*Δ *sfk1*Δ, and *crf1*Δ *lem3*Δ double mutants. Cells were cultured and stained with filipin as in Figure 5A. Bar, 5 μm.

**Supplemental Figure 6**

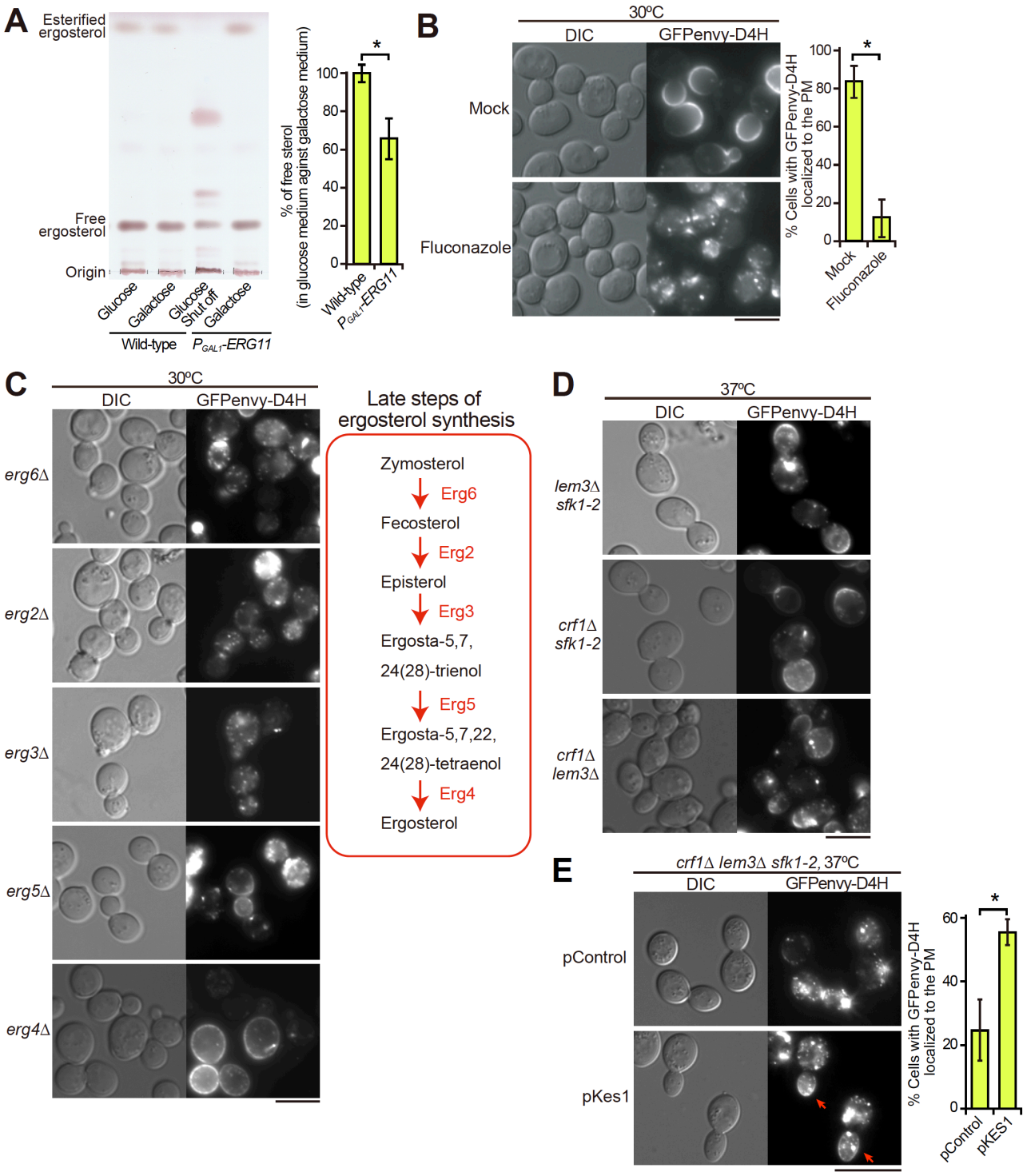


**Supplemental Figure 6.** Ergosterol-dependent PM localization of GFPenvy-D4H. (A) Decrease of free ergosterol by the depletion of Erg11. Cells were cultured as in Figure 5E. Ergosterol contents were analyzed by TLC as described in the "Materials and Methods". *Right panel*: the percentage of free ergosterol of the glucose-cultured cells relative to that of the galactose-cultured cells was determined and is expressed as the mean ± S.D. derived from the analysis of four independent samples. An asterisk indicates a significant difference, as determined by two-tailed Student's t-test ($p < 0.05$). (B) Fluconazole treatment inhibits the GFPenvy-D4H distribution to the PM. Wild-type cells harboring pRS316-GFPenvy-D4H were grown in SDA-Ura medium to the mid-log phase at 30°C and then treated with 100 μM fluconazole or mock treated, followed by incubation for 6 h at 30°C. *Right panel*:

the percentage of cells with GFPenvy-D4H at the PM was determined and is expressed as the mean ± S.D. of three independent experiments (n > 257 cells in total for each condition). An asterisk indicates a significant difference, as determined by two-tailed Student's t-test ($p < 0.05$). (C) The distribution of GFPenvy-D4H in mutants of genes encoding the enzymes in the late steps of ergosterol biosynthesis (*ERG2-6*). Cells were cultured in SDA-Ura medium at 30°C to the mid-log phase. (D) GFPenvy-D4H was localized to the PM in the *lem3*Δ *sfk1-2*, *crf1*Δ *sfk1-2*, and *crf1*Δ *lem3*Δ double mutants. Cells were cultured as in Figure 2E, except that SDA-Ura medium was used. (E) The PM localization of GFPenvy-D4H was partially recovered by *KES1* overexpression in the *crf1*Δ *lem3*Δ *sfk1-2* triple mutant. Cells harboring pRS316-GFPenvy-D4H and either YEplac181-*KES1* or YEplac181 were cultured as in Figure 2E except that SD-Leu-Ura medium was used. Arrows indicate the PM localization of GFPenvy-D4H. *Right panel*: the percentage of cells with GFPenvy-D4H at the PM was determined and is expressed as the mean ± S.D. of three independent experiments (n > 121 in total for each strain). An asterisk indicates a significant difference, as determined by two-tailed Student's t-test ($p < 0.05$). Bars, 5 μm.

**Supplemental Figure 7**

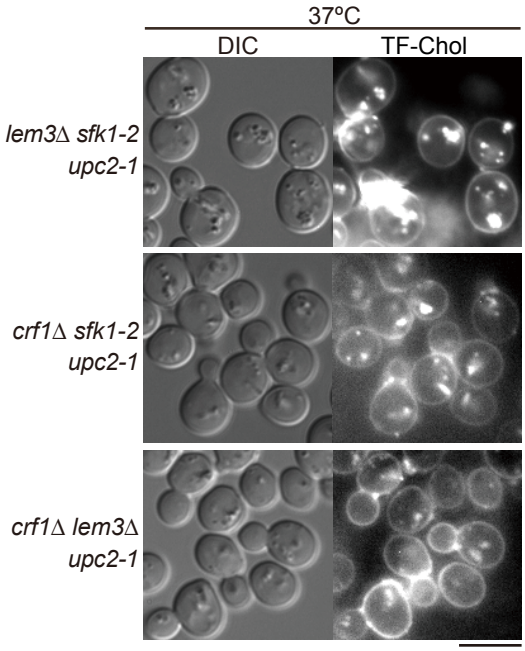


**Supplemental Figure 7.** TF-Chol is retained in the PM of the *lem3*Δ *sfk1-2*, *crf1*Δ *sfk1-2*, and *crf1*Δ *lem3*Δ double mutants. Cells were cultured and labeled with TF-Chol as described in the "Materials and Methods". Bar, 5 μm.

**Supplemental Figure 8**

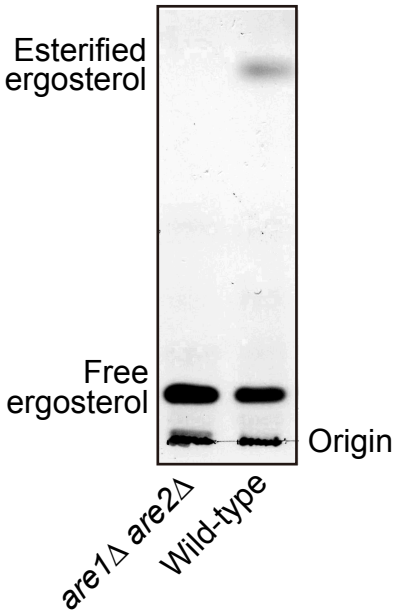


**Supplemental Figure 8.** Identification of esterified ergosterol. TLC analysis of total sterols was performed as in Figure 7A. To detect esterified ergosterol, total lipids were extracted from cells in the stationary phase.

**Supplemental Figure 9**

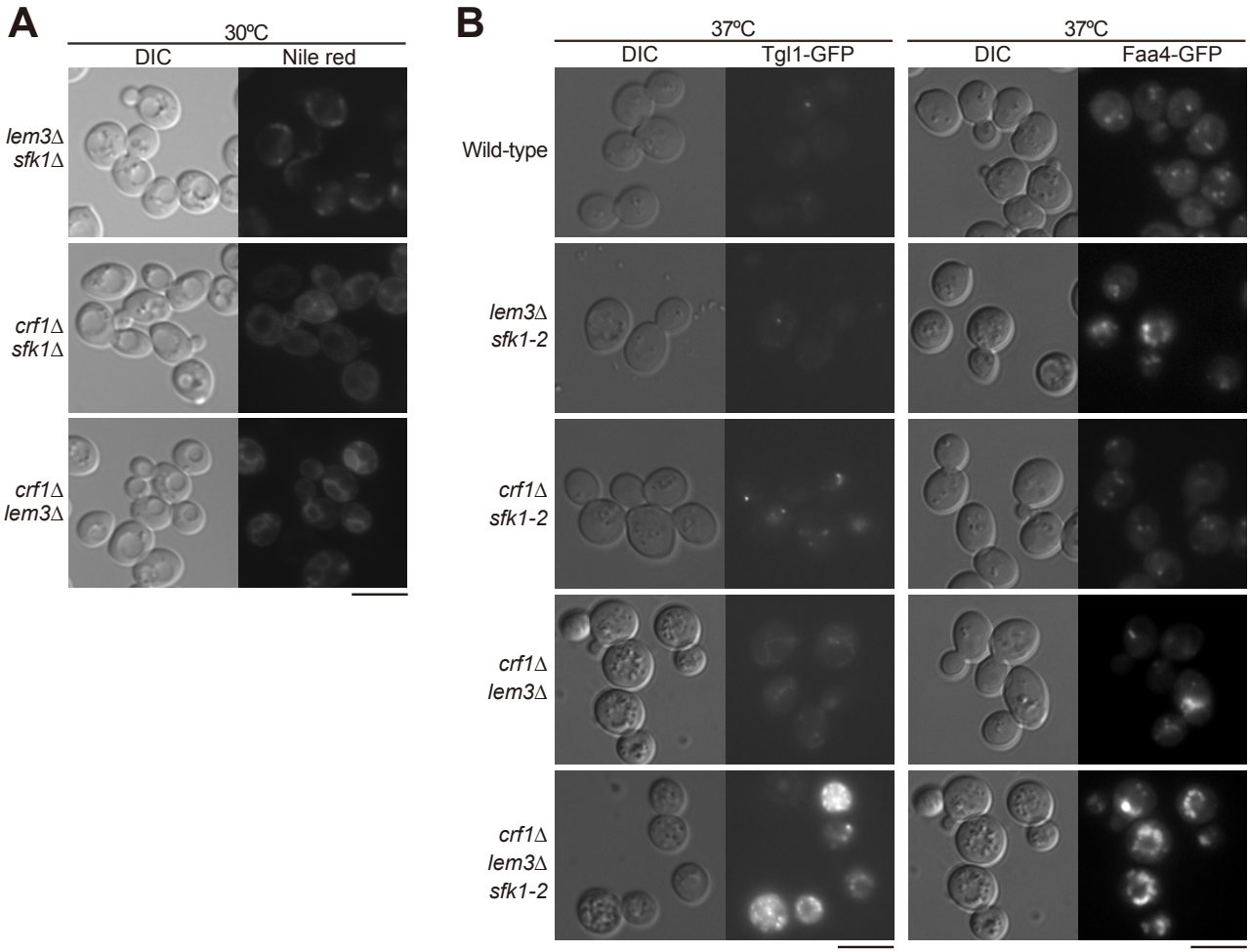


**Supplemental Figure 9.** Lipid droplets are increased in the *crf1*Δ *lem3*Δ *sfk1-2* triple mutant. (A) Nile red staining in the *lem3*Δ *sfk1*Δ, *crf1*Δ *sfk1*Δ, and *crf1*Δ *lem3*Δ double mutants. Cells were cultured in YPDA medium to the mid-log phase at 30°C, followed by Nile red staining. Nile red staining was performed as described in the "Materials and Methods". (B) Accumulation of Tgl1-GFP (left) and Faa4-GFP (right) puncta in the *crf1*Δ *lem3*Δ *sfk1-2* triple mutant. Cells were cultured as in Figure 2E. All images were acquired and processed under the same conditions for comparison of fluorescence intensity. Bars, 5 μm.

**Supplemental Figure 10**

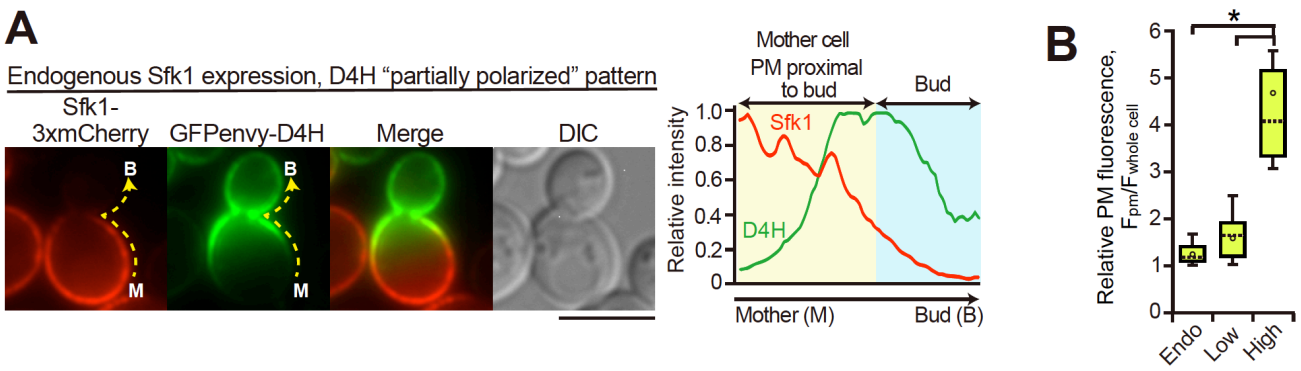


**Supplemental Figure 10.** Classification of Sfk1-mCherry-expressing cells with low or high expression patterns. (A) Fluorescence intensity profile of a cell showing the "partially polarized" pattern of GFPenvy-D4H. Fluorescence signals were quantified along the dotted line from the mother cell to the bud. The brightness of Sfk1-3xmCherry was adjusted as in Figure 9B. Bar, 3 µm. (B) Classification of Sfk1-mCherry-expressing cells with low or high expression patterns. The cells in Figure 9E were examined. Low or high expression of Sfk1-mCherry was determined for each cell on the basis of our threshold value, which was set at 300% of the fluorescence intensity of endogenously expressed Sfk1-3xmCherry. Fluorescence intensity at the PM was quantitated as described in the "Materials and Methods". The ratio of the fluorescence at the PM ($F_{pm}$)/that of whole cell ($F_{whole\ cell}$) was determined and expressed with a boxplot (whiskers: maximum and minimum values; box: first quartile, median, and third quartile; circle: average). *Bars*: Endo, endogenous expression of Sfk1-3xmCherry; Low, multicopy plasmid of *SFK1-mCherry* but low expression of Sfk1-mCherry; High, multicopy plasmid of *SFK1-mCherry* and high expression of Sfk1-mCherry. The numbers of cells analyzed were 13, 34, and 22 for Endo, Low, and High, respectively. An asterisk indicates a significant difference, as determined by the Tukey–Kramer test ($p < 0.05$).

**Supplemental Table 1.** *S. cerevisiae* strains used in this study

| Strain[a,b] | Mating type | Genotype | Reference or source |
|---|---|---|---|
| YKT38 | a | Wild-type (*lys2-801 ura3-52 his3Δ-200 trp1Δ-63 leu2Δ-1*) | (Misu *et al.*, 2003) |
| YKT715 | a | *lem3Δ::TRP1* | (Saito *et al.*, 2004) |
| YKT2329 | a | *crf1Δ::HphMX4* | This study |
| YKT2117 | a | *sfk1Δ::KanMX6* | (Mioka *et al.*, 2018) |
| YKT2330 | a | *lem3Δ::TRP1 sfk1Δ::KanMX6* | This study |
| YKT2331 | a | *crf1Δ::HphMX4 sfk1Δ::KanMX6* | This study |
| YKT2332 | α | *crf1Δ::HphMX4 lem3Δ::TRP1* | This study |
| YKT2333 | a | *crf1Δ::HphMX4 lem3Δ::TRP1 sfk1Δ::KanMX6* | This study |
| YKT2334 | α | *dnf3Δ::HIS3MX6 sfk1Δ::KanMX6* | This study |
| YKT783 | a | *CRF1-GFP::KanMX6* | This study |
| YKT1412 | α | *vrp1Δ::LUE2 CRF1-GFP::KanMX6* | This study |
| YKT2335 | a | *DNF3-3xGFP::CaURA3* | This study |
| YKT2336 | a | *vrp1Δ::LUE2 DNF3-3xGFP::CaURA3* | This study |
| YKT2337 | a | *sfk1-2::KlLEU2* | This study |
| YKT2338 | a | *lem3Δ::TRP1 sfk1-2::KlLEU2* | This study |
| YKT2339 | a | *crf1Δ::HphMX4 sfk1-2::KlLEU2* | This study |
| YKT2340 | a | *crf1Δ::HphMX4 lem3Δ::TRP1 sfk1-2::KlLEU2* | This study |
| YKT917 | α | *dnf3Δ::HIS3MX6* | This study |
| YKT2341 | a | *dnf3Δ::HIS3MX6 lem3Δ::TRP1* | This study |
| YKT2343 | a | *URA3::GFP-Lact-C2* | (Takeda *et al.*, 2014) |
| YKT2344 | a | *lem3Δ::TRP1 sfk1-2::KlLEU2 URA3::GFP-Lact-C2* | This study |
| YKT2345 | a | *crf1Δ::HphMX4 sfk1-2::KlLEU2 URA3::GFP-Lact-C2* | This study |
| YKT2346 | a | *crf1Δ::HphMX4 lem3Δ::TRP1 URA3::GFP-Lact-C2* | This study |
| YKT2347 | a | *crf1Δ::HphMX4 lem3Δ::TRP1 sfk1-2::KlLEU2 URA3::GFP-Lact-C2* | This study |
| YKT2348 | a | *URA3::GFP-evt-2PH* | This study |
| YKT2349 | a | *lem3Δ::TRP1 sfk1-2::KlLEU2 URA3::GFP-evt-2PH* | This study |
| YKT2350 | a | *crf1Δ::HphMX4 sfk1-2::KlLEU2 URA3::GFP-evt-2PH* | This study |
| YKT2351 | a | *crf1Δ::HphMX4 lem3Δ::TRP1 URA3::GFP-evt-2PH* | This study |
| YKT2352 | a | *crf1Δ::HphMX4 lem3Δ::TRP1 sfk1-2::KlLEU2 URA3::GFP-evt-2PH* | This study |
| YKT2354 | a | *URA3::GFP-SNC1* | (Zendeh-boodi *et al.*, 2013) |
| YKT2355 | a | *crf1Δ::HphMX4 lem3Δ::TRP1 sfk1-2::KlLEU2 URA3::GFP-SNC1* | This study |

*Continued*

**Supplemental Table 1** *Continued*

| Strain[a,b] | Mating type | Genotype | Reference or source |
|---|---|---|---|
| YKT1187 | a | *PDR5-GFP::KanMX6* | This study |
| YKT2356 | a | *crf1Δ::HphMX4 lem3Δ::TRP1 sfk1-2::KlLEU2 PDR5-GFP::KanMX6* | This study |
| YKT2357 | a | *VPH1-3xGFP::CaURA3* | This study |
| YKT2358 | a | *crf1Δ::HphMX4 lem3Δ::TRP1 sfk1-2::KlLEU2 VPH1-3xGFP::CaURA3* | This study |
| YKT2400 | a | *HIS3MX6::$P_{GAL1}$-3HA-ERG11* | This study |
| YKT2119 | a | *erg6Δ::KanMX6 TRP1* | (Mioka *et al.*, 2018) |
| YKT2401 | a | *erg2Δ::TRP1* | This study |
| KKT12 | a | *erg3Δ::HphMX4 TRP1* | (Kishimoto *et al.*, 2005) |
| YKT2402 | a | *erg5Δ::HIS3MX6* | This study |
| KKT252 | a | *erg4Δ::HphMX4 TRP1* | (Kishimoto *et al.*, 2005) |
| YKT2403 | α | *URA3::upc2-1* | This study |
| YKT2404 | a | *lem3Δ::TRP1 sfk1-2::NatMX6 URA3::upc2-1* | This study |
| YKT2405 | a | *crf1Δ::HphMX4 sfk1-2::NatMX6 URA3::upc2-1* | This study |
| YKT2406 | a | *crf1Δ::HphMX4 lem3Δ::TRP1 URA3::upc2-1* | This study |
| YKT2407 | a | *crf1Δ::HphMX4 lem3Δ::TRP1 sfk1-2::NatMX6 URA3::upc2-1* | This study |
| YKT2408 | a | *TGL1-GFP::CaURA3* | This study |
| YKT2409 | a | *lem3Δ::TRP1 sfk1-2::KlLEU2 TGL1-GFP::CaURA3* | This study |
| YKT2410 | a | *crf1Δ::HphMX4 sfk1-2::KlLEU2 TGL1-GFP::CaURA3* | This study |
| YKT2411 | a | *crf1Δ::HphMX4 lem3Δ::TRP1 TGL1-GFP::CaURA3* | This study |
| YKT2412 | a | *crf1Δ::HphMX4 lem3Δ::TRP1 sfk1-2::KlLEU2 TGL1-GFP::CaURA3* | This study |
| YKT2413 | a | *FAA4-GFP::CaURA3* | This study |
| YKT2414 | a | *lem3Δ::TRP1 sfk1-2::KlLEU2 FAA4-GFP::CaURA3* | This study |
| YKT2415 | a | *crf1Δ::HphMX4 sfk1-2::KlLEU2 FAA4-GFP::CaURA3* | This study |
| YKT2416 | a | *crf1Δ::HphMX4 lem3Δ::TRP1 FAA4-GFP::CaURA3* | This study |
| YKT2417 | a | *crf1Δ::HphMX4 lem3Δ::TRP1 sfk1-2::KlLEU2 FAA4-GFP::CaURA3* | This study |
| YKT2418 | a | *FAA4-mCherry::KanMX6 URA3::upc2-1* | This study |
| YKT2419 | a | *crf1Δ::HphMX4 lem3Δ::TRP1 sfk1-2::KlLEU2 FAA4-mCherry::KanMX6 URA3::upc2-1* | This study |
| YKT2420 | a | *are1Δ::KanMX6* | This study |
| YKT2421 | a | *are2Δ::HIS3MX6* | This study |
| YKT2422 | a | *crf1Δ::HphMX4 lem3Δ::TRP1 sfk1-2::KlLEU2 are1Δ::KanMX6* | This study |

*Continued*

**Supplemental Table 1** *Continued*

| Strain[a,b] | Mating type | Genotype | Reference or source |
|---|---|---|---|
| YKT2423 | a | *crf1Δ::HphMX4 lem3Δ::TRP1 sfk1-2::KlLEU2 are2Δ::HIS3MX6* | This study |
| YKT2428 | a | *SFK1-3xmCherry::KanMX6* | This study |

[a] YKT strains are isogenic derivatives of YEF473 (Longtine *et al.*, 1998). Only relevant genotypes are described.
[b] KKT12 and KKT252 strains are isogenic derivatives of BY4743 (Brachmann *et al.*, 1998).

**Reference**

Brachmann, C.B., Davies, A., Cost, G.J., Caputo, E., Li, J., Hieter, P., and Boeke, J.D. (1998). Designer deletion strains derived from Saccharomyces cerevisiae S288C: a useful set of strains and plasmids for PCR-mediated gene disruption and other applications. Yeast *14*, 115-132.

Kishimoto, T., Yamamoto, T., and Tanaka, K. (2005). Defects in structural integrity of ergosterol and the Cdc50p-Drs2p putative phospholipid translocase cause accumulation of endocytic membranes, onto which actin patches are assembled in yeast. Mol Biol Cell *16*, 5592-5609.

Longtine, M.S., McKenzie, A., 3rd, Demarini, D.J., Shah, N.G., Wach, A., Brachat, A., Philippsen, P., and Pringle, J.R. (1998). Additional modules for versatile and economical PCR-based gene deletion and modification in Saccharomyces cerevisiae. Yeast *14*, 953-961.

Mioka, T., Fujimura-Kamada, K., Mizugaki, N., Kishimoto, T., Sano, T., Nunome, H., Williams, D.E., Andersen, R.J., and Tanaka, K. (2018). Phospholipid flippases and Sfk1p,

a novel regulator of phospholipid asymmetry, contribute to low permeability of the plasma membrane. Mol Biol Cell *29*, 1203-1218.

Misu, K., Fujimura-Kamada, K., Ueda, T., Nakano, A., Katoh, H., and Tanaka, K. (2003). Cdc50p, a conserved endosomal membrane protein, controls polarized growth in Saccharomyces cerevisiae. Mol Biol Cell *14*, 730-747.

Saito, K., Fujimura-Kamada, K., Furuta, N., Kato, U., Umeda, M., and Tanaka, K. (2004). Cdc50p, a protein required for polarized growth, associates with the Drs2p P-type ATPase implicated in phospholipid translocation in Saccharomyces cerevisiae. Mol Biol Cell *15*, 3418-3432.

Takeda, M., Yamagami, K., and Tanaka, K. (2014). Role of phosphatidylserine in phospholipid flippase-mediated vesicle transport in Saccharomyces cerevisiae. Eukaryot Cell *13*, 363-375.

Zendeh-boodi, Z., Yamamoto, T., Sakane, H., and Tanaka, K. (2013). Identification of a second amphipathic lipid-packing sensor-like motif that contributes to Gcs1p function in the early endosome-to-TGN pathway. J Biochem *153*, 573-587.

**Supplemental Table 2.** Plasmids used in this study

| Plasmid | Characteristics | Reference or source |
|---|---|---|
| YEplac195 | *URA3 2μm* | (Gietz and Sugino, 1988) |
| YEplac181 | *LEU2 2μm* | (Gietz and Sugino, 1988) |
| pRS306 | *URA3* | (Sikorski and Hieter, 1989) |
| pRS316 | *URA3 CEN* | (Sikorski and Hieter, 1989) |
| pRS315 | *LEU2 CEN* | (Sikorski and Hieter, 1989) |
| pBluescript II SK+ | | (Alting-Mees and Short, 1989) |
| pKT2210 [pRS316-*SFK1*] | *SFK1 URA3 CEN* | This study |
| pKT2180 [pRS315-*SFK1*] | *SFK1 LEU2 CEN* | This study |
| pKT1252 [pRS315-*LEM3*] | *LEM3 LEU2 CEN* | (Kishimoto *et al.*, 2005) |
| pKT2211 [pRS315-*CRF1*] | *CRF1 LEU2 CEN* | This study |
| pKT2212 [YEplac195-*OSH2*] | *OSH2 URA3 2μm* | This study |
| pKT2213 [YEplac195-*OSH3*] | *OSH3 URA3 2μm* | This study |
| pKT2175 [YEplac195-*KES1*] | *KES1 URA3 2μm* | This study |
| pKT2114 [YEplac195- $KES1^{E117A}$] | $KES1^{E117A}$ *URA3 2μm* | This study |
| pKT2115 [YEplac195- $KES1^{L111D}$] | $KES1^{L111D}$ *URA3 2μm* | This study |
| pKT2116 [YEplac195- $KES1^{Y97F}$] | $KES1^{Y97F}$ *URA3 2μm* | This study |
| pKT2217 [YEplac195-*OSH5*] | *OSH5 URA3 2μm* | This study |
| pKT2218 [YEplac195-*OSH6*] | *OSH6 URA3 2μm* | This study |
| pKT2219 [YEplac195-*OSH7*] | *OSH7 URA3 2μm* | This study |
| pKT2220 [pRS316-GFP-D4H] | $P_{TPI1}$*-GFP-D4H URA3 CEN* | This study |
| pKT2221 [pRS316-GFPenvy-D4H] | $P_{TPI1}$*-GFPenvy-D4H URA3 CEN* | This study |
| pKT2017 [YEplac181-*KES1*] | *KES1 LEU2 2μm* | This study |
| pKT2222 [pBluescript II SK+-*DNF3-3xGFP*] | *DNF3-Cterminal-3xGFP CaURA3* | This study |
| pKT2224 [pBluescript II SK+-*VPH1-3xGFP*] | *VPH1-Cterminal-3xGFP CaURA3* | This study |
| pKT2225 [pBluescript II SK+-S*FK1-3xmCherry*] | *SFK1-Cterminal-3xmCherry CaURA3* | This study |
| pKT2226 [pRS306-*GFP-evt2-2PH*] | $P_{TPI1}$*-GFP-evt2-2PH URA3* | This study |
| pKT2227 [YEplac181-*SFK1-mCherry*] | *SFK1-mCherry LEU2 2μm* | This study |
| pKT2228 [pRS306-*upc2-1*] | *upc2-1 URA3* | This study |
| pKT2230 [YEplac195-*KanMX6*] | *KanMX6 URA3 2μm* | This study |
| pKT2231 [YEplac195-*KES1-KanMX6*] | *KES1 KanMX6 URA3 2μm* | This study |
| pKT2232 [pColdI-GFP-D4H] | GFP-D4H | This study |
| pKT2233 [pColdI-GFPenvy-D4H] | GFPenvy-D4H | This study |

**Reference**

Alting-Mees, M.A., and Short, J.M. (1989). pBluescript II: gene mapping vectors. Nucleic Acids Res *17*, 9494.

Gietz, R.D., and Sugino, A. (1988). New yeast-Escherichia coli shuttle vectors

constructed with in vitro mutagenized yeast genes lacking six-base pair restriction sites. Gene *74*, 527-534.

Kishimoto, T., Yamamoto, T., and Tanaka, K. (2005). Defects in structural integrity of ergosterol and the Cdc50p-Drs2p putative phospholipid translocase cause accumulation of endocytic membranes, onto which actin patches are assembled in yeast. Mol Biol Cell *16*, 5592-5609.

Sikorski, R.S., and Hieter, P. (1989). A system of shuttle vectors and yeast host strains designed for efficient manipulation of DNA in Saccharomyces cerevisiae. Genetics *122*, 19-27.